Structural properties of Au and Ag nanoclusters embedded in MgO

Fedorov, A.V.; Veen, A. van; Falub, C.V.; Eijt, S.W.H.; Kooi, B.J.; Hosson, J.Th.M. De; Hibma, T.; Zimmerman, R.L.

Published in:
Nuclear Instruments & Methods in Physics Research Section B-Beam Interactions with Materials and Atoms

DOI:
10.1016/S0168-583X(02)00589-X

Publication date:
2002

ELSEVIER

Nuclear Instruments and Methods in Physics Research B 191 (2002) 442–446

NIM B
Beam Interactions with Materials & Atoms

www.elsevier.com/locate/nimb

Structural properties of Au and Ag nanoclusters embedded in MgO

M.A. van Huis [a,*], A.V. Fedorov [a], A. van Veen [a], C.V. Falub [a], S.W.H. Eijt [a], B.J. Kooi [b], J.Th.M. De Hosson [b], T. Hibma [b], R.L. Zimmerman [c]

[a] *Interfaculty Reactor Institute, Delft University of Technology, Mekelweg 15, NL 2629 JB Delft, The Netherlands*
[b] *Materials Science Center, University of Groningen, Nijenborg 4, NL 9747 AG Groningen, The Netherlands*
[c] *Center of Irradiation of Materials, Alabama A&M University, AL 35762-1447, USA*

Abstract

Gold and silver nanoclusters embedded in MgO were created by means of ion implantation of 1.0 MeV Au or 600 keV Ag ions to a dose of 10^{16} cm^{-2} into single crystals of MgO(1 0 0) and subsequent annealing at 1473 K for a period of 22 h. The structural properties of the nanoclusters were characterised by optical absorption spectroscopy (OAS), high-resolution X-ray diffraction (XRD) and cross-sectional transmission electron microscopy (XTEM). Nanocluster sizes are estimated using three different methods: using the Doyle formula for the broadening of the optical absorption peak associated with Mie plasmon resonance; using the Scherrer formula for the broadening of the Au and Ag XRD peaks, and from direct observation of TEM images. For the Au clusters, the methods are in excellent agreement with mean cluster sizes of 4–5 nm. For the Ag clusters, the optical Doyle method yields a mean nanocluster size of 5 nm while the XRD and XTEM methods yield 10–11 nm. The XRD and XTEM results reveal a cube-on-cube orientation relationship of the Au and Ag nanoclusters with respect to the MgO matrix.

Keywords: Ion implantation; Nanoclusters; Electron microscopy; X-ray diffraction

1. Introduction

Metal and semiconductor nanoclusters embedded in transparent matrices exhibit linear and non-linear optical properties that are of interest to the field of opto-electronics [1,2]. A feasible way of producing these clusters is by means of ion implantation and subsequent annealing [3,4]. Unless the implantation doses are very high, the precipitation of the implanted atoms starts only after subsequent annealing. Many factors influence the size and the size distribution of these precipitates, such as the ion implantation dose, the ion implantation energy, the annealing temperature, the annealing time and the chemical environment where the annealing takes place (inert, oxidising or reducing environment). The average size and the size distribution are best determined from cross-sectional transmission electron microscopy (XTEM). However, this technique often implies destruction of the sample and the specimen preparation is time consuming. Therefore, many authors working on annealing studies try to estimate

* Corresponding author. Tel.: +31-152-781612; fax: +31-152-786422.
E-mail address: vanhuis@iri.tudelft.nl (M.A. van Huis).

0168-583X/02/$ - see front matter
PII: S0168-583X(02)00589-X

the precipitate size from the broadening of the optical absorption peak that is present as a result of Mie plasmon resonance [4]. Here the Doyle theory [5] is used to estimate the nanocluster size during the annealing procedure. Alternatively, the size can be estimated from the broadening of the XRD diffraction peaks using the Scherrer formula [6]. In this work, we compare the nanocluster size as obtained from the three methods mentioned above. XRD and XTEM are also employed in order to determine the coherency and the orientation relationship of the gold clusters with the surrounding matrix.

2. Experimental

In order to create silver and gold nanoclusters, epipolished MgO(1 0 0) single crystals of size $10 \times 10 \times 1$ mm^3 were implanted at room temperature with 1.0×10^{16} Au or Ag ions cm^{-2} at an energy of 1.0 MeV and 600 keV, respectively. These energies were chosen in order to obtain the same ion distribution depth so that the atomic concentration of implanted species in the ion implanted layer is approximately equal for both Au and Ag as predicted by the TRIM ion implantation code [7]. After ion implantation, the samples were annealed in ambient air at temperatures up to 1473 K for a period of 22 h. The sample treatment data are listed in Table 1. The following techniques have been employed for the characterisation of the optical and structural properties of the nanoclusters: optical absorption spectroscopy (OAS), high-resolution X-ray diffraction (XRD) and XTEM. The XRD measurements were performed using a Philips X'Pert materials research diffractometer system; a ceramic X-ray tube provided Cu K_α radiation. The TEM was performed using a JEOL 4000 EX/II operating at 400 kV (point-to-point resolution 0.17 nm). The specimen preparation is discussed elsewhere [8].

3. Results

The results of the optical absorption measurements carried out on the MgO:Au and MgO:Ag samples have already been published previously [7] and here we will only present the results of Doyle for the analysis of the Mie plasmon resonance peak. In the Doyle theory, the free mean path of the electrons constituting the plasmon is limited by the size of the nanocluster. This allows estimation of the cluster size as [5]

$$D = 2\frac{v_F}{\Delta\omega_{1/2}} = 2\frac{v_F}{2\pi c}\frac{\lambda_{max}^2}{\Delta\lambda_{1/2}}. \quad (1)$$

Here D is the diameter of the precipitate (m), v_F the Fermi velocity (1.39×10^6 m s^{-1} both for gold and silver [9]), $\Delta\omega_{1/2}$ the FWHM of the peak when plotted as a function of the circular frequency ω (rad s^{-1}), c the speed of light (m s^{-1}), λ_{max} the position of the centroid of the peak and $\Delta\lambda_{1/2}$ is the FWHM of the peak when plotted as a function of wavelength (m). The background in the optical spectra was fitted with an exponential function and the Mie plasmon resonance peak was fitted with a Gaussian. The FWHM of the Gaussian and the parameters mentioned above were substituted in Eq. (1), yielding cluster diameters of 4.3 and 5.1 nm for the Au and Ag clusters, respectively.

Table 1
Sample treatment and structural properties of the Au and Ag nanoclusters

	MgO:Au	MgO:Ag
Sample treatment		
Implantation	1 MeV, 10^{16} Au^+ cm^{-2}	600 keV, 10^{16} Ag^+ cm^{-2}
Thermal anneal	1473 K, 22 h	1473 K, 22 h
Cluster size and shape		
Optical absorption, Doyle (nm)	4.3	5.1
XRD (Scherrer), (1 1 3) peak	4.0 nm ($K_w = 0.8290$)	9.8 nm ($K_w = 0.8863$)
XTEM		
Mean size (nm)	4.6	11
Distribution (nm)	2–14	6–24
Shape	Spherical	Octahedral
Lattice parameter a		
Literature	4.078 Å	4.085 Å
Misfit ($a_{MgO} = 4.212$ Å)	3.2%	3.0%
Experimental a (XRD)	4.09 Å	4.12 Å
Coherency strain $\varepsilon_{[1\,0\,0]}$ (XRD)	+0.4%	+0.9%

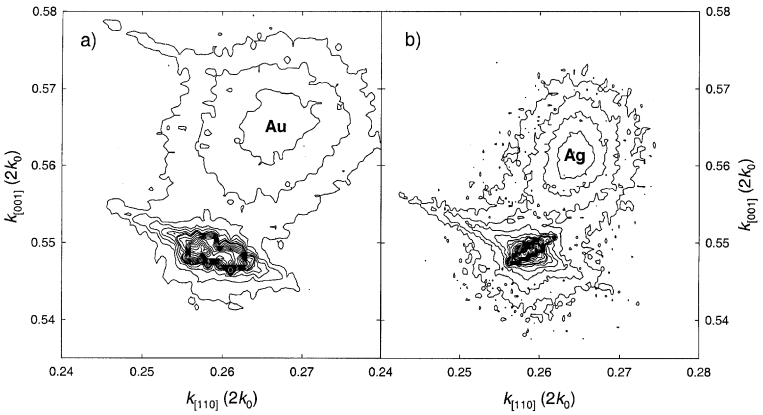

Fig. 1. Reciprocal space plots of (a) the MgO(1 1 3) and Au(1 1 3) diffraction peaks of the MgO:Au sample and (b) the MgO(1 1 3) and Ag(1 1 3) diffraction peaks of the MgO:Ag sample. Units are in $2k_0 = 2/\lambda_0$.

High-resolution XRD measurements were carried out on the MgO(0 0 2), (1 1 3), (0 0 4) and (0 2 4) diffraction peaks. Figs. 1(a) and (b) show the contour plots of the (1 1 3) diffraction peaks of the MgO:Au and MgO:Ag samples. The $k_{[1\,1\,0]}$ axis corresponds to diffraction along the [0 0 1] crystal axis (perpendicular to the surface) and the $k_{[1\,1\,0]}$ axis corresponds to diffraction along the [1 1 0] crystal axis (parallel to the surface). The crystal structure of MgO, Au and Ag is fcc and their lattice parameters are listed in Table 1. Because the lattice parameters of Au and Ag are close to that of MgO, Au(1 1 3) and Ag(1 1 3) satellite peaks are observed near the intense MgO(1 1 3) peaks in Fig. 1. The broadening of the MgO diffraction peaks is due to mosaic broadening (rocking curve). The Au and Ag satellite peaks were also found near the MgO-(0 0 2), (0 0 4) and (0 2 4) diffraction peaks, clearly indicating a cube-on-cube orientation relationship with the MgO host matrix. The cluster size was estimated from the width of the (0 0 2) and (1 1 3) diffraction peaks using the Scherrer formula [6]

$$p = K_{\mathrm{w}} \frac{\lambda_0}{\Delta\vartheta \cos\vartheta} = K_{\mathrm{w}} \frac{2}{\Delta k \sqrt{h^2 + k^2 + l^2}}. \qquad (2)$$

Here p is the precipitate size, defined as the cube root of the precipitate volume. Furthermore, λ_0 is the wavelength (1.540560 Å), ϑ the position of the $(h\,k\,l)$ diffraction peak, $\Delta\vartheta$ the FWHM of the same diffraction peak and Δk the FWHM of the peak in reciprocal space in m^{-1}. The half-width Scherrer constant K_{w} depends on the shape of the nanocluster and if the clusters are not spherically shaped also on the $(h\,k\,l)$ index of the diffraction peak [6]. The right-hand side of Eq. (2) is derived from Bragg's law, $\lambda = 2d_{h\,k\,l}\sin(\vartheta)$ and $k \equiv 1/d_{h\,k\,l}$. Here $d_{h\,k\,l} = d/\sqrt{h^2 + k^2 + l^2}$, where d is the lattice parameter of the material, k is the diffraction vector in reciprocal space and is commonly expressed in units of $2k_0 \equiv 2/\lambda_0$.

The results of the Scherrer analysis are shown in Table 1. From the XTEM results discussed below, it was found that the shape of the Au clusters is spherical and the shape of the Ag clusters is octahedral. The corresponding values for the Scherrer constant K_{w} are listed in Table 1 and obtained from Ref. [6]. The cluster sizes were derived from the (1 1 3) diffraction peaks rather than from the (0 0 2) diffraction peaks, because the diffraction peaks of Au and Ag are better resolved from the MgO diffraction peak in the (1 1 3) case when compared to the (0 0 2) case. Therefore, the cluster sizes as obtained from the (1 1 3) are more accurate. From the positions of the Au(0 0 2) and Ag(0 0 2) peaks, the mean lattice parameter of the nanoclusters perpendicular to the surface was also calculated. It was found that the Au and Ag lattices are extended by 0.4% and 0.9%, respectively, in the direction perpendicular to the surface. This is probably caused by coherency strains, since the lattice parameters of Au and Ag are smaller than the lattice parameter of MgO (see Table 1). Cal-

culation of the tensile strain from the (1 1 3) diffraction peaks yields the same result. We will now discuss the results of the XTEM analysis so that the results of the three methods can be compared.

The MgO:Au and MgO:Ag samples were analysed with XTEM. In the MgO:Au specimen, a band of Au clusters was found in a depth range of about 140–300 nm below the surface. Fig. 2 shows a typical size distribution of the spherically shaped Au clusters. The size of the gold clusters varies from 2 to 14 nm with a mean size of 4.6 nm (average obtained from 40 clusters). Fig. 3 shows a high-resolution TEM (HR TEM) image of a few gold clusters. The cube-on-cube orientation relationship is clearly observable as the lines of the MgO lattice spacing continue in the Au nanocluster. XTEM analysis of the MgO:Ag sample yields a depth range of 180–350 nm below the surface, a size distribution of 6–24 nm and a mean cluster size of 11 nm (average obtained from 75 clusters). Here it was observed that the clusters have octahedral shapes except for the smallest clusters, which have spherical shapes.

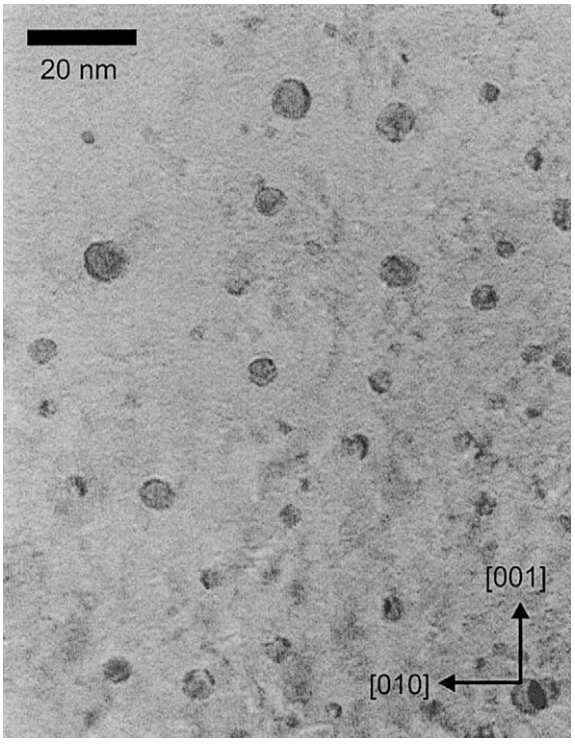

Fig. 2. Bright-field TEM image of a part of the Au implanted layer showing a typical size distribution of spherically shaped Au clusters.

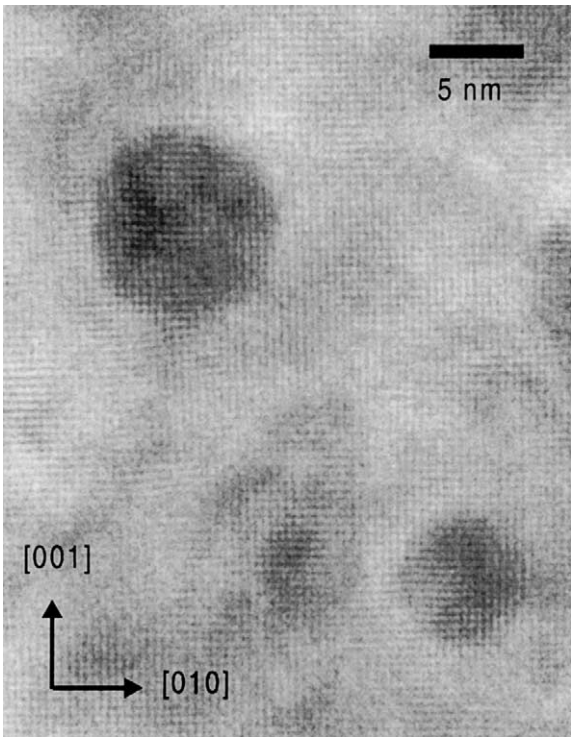

Fig. 3. HR TEM image of a few gold clusters in a cube-on-cube orientation relationship with the embedding MgO matrix.

4. Discussion and conclusions

In determining the mean cluster size, the Scherrer XRD method and the TEM observations are in excellent agreement. In the case of the Ag clusters, the Doyle optical method underestimates the cluster size, which might be attributed to additional broadening due to interface effects. Kreibig et al. [10] have shown that embedding of Ag nanoclusters in various matrices leads to additional broadening of the absorption peaks by a factor of 2–4 when compared to absorption peaks of Ag nanoclusters that are not embedded in a matrix, where the additional broadening is dependent on the embedding medium. Contemplating Eq. (1), additional broadening of $\Delta\lambda_{1/2}$ leads to an

underestimation of the cluster size. XRD and TEM do not suffer from this artifact. However, both the Doyle method and the Scherrer method may suffer from the effect of size distribution, which, in general, also induces additional broadening. Nevertheless, the results shown in Table 1 show that the Scherrer method still accurately predicts the mean cluster size as observed by means of TEM. It was found here that from these three methods to determine the cluster size, the Doyle optical method is the least accurate. This is caused by the asymmetry of the absorption peaks, inaccurate background subtraction and systematic underestimation due to interface effects. Scherrer XRD and XTEM are both accurate methods to determine the mean cluster size, where XTEM can also provide a good indication of the cluster size distribution. Considering that optical measurements take typically 10 min, XRD measurements a few hours and XTEM measurements about 3 days (including specimen preparation), Scherrer XRD is probably the best compromise. However if one is interested mainly in the optical properties important for applications, optical absorption studies are indispensable.

References

[1] P. Chakraborty, J. Mater. Sci. 33 (1998) 2235.
[2] K. Fukumi, A. Chayahara, K. Kodano, T. Sakaguchi, Y. Horino, M. Miya, K. Jujii, J. Hayakawa, M. Satou, J. Appl. Phys. 75 (6) (1994) 3075.
[3] C.W. White, J.D. Budai, S.P. Withrow, J.G. Zhu, E. Sonder, R.A. Zuhr, A. Meldrum, D.M. Hembree Jr., D.O. Henderson, S. Prawer, Nucl. Instr. and Meth. B 141 (1998) 228.
[4] R.L. Zimmerman, D. Ila, E.K. Williams, D.B. Poker, D.K. Hensley, C. Klatt, S. Kalbitzer, Nucl. Instr. and Meth. B 148 (1999) 1064 (and references therein).
[5] W.T. Doyle, Phys. Rev. 111 (4) (1958) 1067.
[6] J.I. Langford, A.J.C. Wilson, J. Appl. Cryst. 11 (1978) 102.
[7] A.V. Fedorov, A. van Veen, M.A. van Huis, H. Schut, B.J. Kooi, J.Th.M. De Hosson, R.L. Zimmerman, in: Conference Proceedings of CAARI 2000, Denton.
[8] B.J. Kooi, A. van Veen, J.Th.M. de Hosson, H. Schut, A.V. Fedorov, F. Labohm, Appl. Phys. Lett. 76 (9) (2000) 1110.
[9] C. Kittel, Introduction to Solid State Physics, 6th ed., John Wiley & Sons, New York, 1986, p. 134.
[10] U. Kreibig, A. Hilger, H. Hövel, M. Quinten, in: T.P. Martin (Ed.), Large Clusters of Atoms and Molecules, Kluwer Academic Publishers, Dordrecht, Netherlands, 1996, p. 475.